

# A HIGH-ORDER QUADRATURE METHOD FOR IMPLICITLY DEFINED HYPERSURFACES AND REGIONS

ZIBO ZHAO \*

**Abstract.** This paper presents a high-order accurate numerical quadrature algorithm for evaluating integrals over curved surfaces and regions defined implicitly via a level set of a given function restricted to a hyperrectangle. The domain is divided into small tetrahedrons, and by employing the change of variables formula, the approach yields an algorithm requiring only one-dimensional root finding and standard Gaussian quadrature. The resulting quadrature scheme guarantees strictly positive weights and inherits the high-order accuracy of Gaussian quadrature. Numerical convergence tests confirm the method’s high-order accuracy.

**Keywords.** high-order quadrature, implicit surfaces, level set function

**1. Introduction** This paper develops a high-order numerical quadrature method for computing integrals over hypersurfaces defined implicitly as the zero level set of a smooth function  $F : \mathbb{R}^d \rightarrow \mathbb{R}$ . Let  $\Gamma = \{x : F(x) = 0\}$  denote the hypersurface and  $\Omega = \{x : F(x) \leq 0\}$ . Specifically, we consider the surface integral

$$\int_{\Gamma \cap U} f dS,$$

and the region integral

$$\int_{\Omega \cap U} f dx,$$

where  $U \subset \mathbb{R}^d$  is a hyperrectangle (e.g.,  $\prod_{i=1}^d [a_i, b_i]$ ), with  $\nabla F$  non-vanishing on  $\Gamma$ , and both  $F$  and  $f$  assumed smooth.

Several high-order methods for integration on implicitly defined domains exist. One approach resolves the geometry through approximation; for instance, [6] presents a method dividing the domain into tetrahedra and reconstructing the surface via piecewise linear interpolation. Similarly, [5] achieves high-order accuracy using surface reconstruction techniques like marching cubes or marching tetrahedra [15, 11]. Another approach multiplies the integrand by delta or Heaviside functions. As these functions are discontinuous, regularization becomes necessary. Works such as [7, 13, 14, 19] demonstrate that suitable regularized functions yield first- or second-order schemes, while [16, 17, 18] derive higher-order discretizations. Related techniques extend the integration domain using the coarea formula [3]. Moment-fitting methods provide another alternative, directly discretizing the quadrature rule and solving for coefficients via moment-fitting equations [9, 8]. Although computationally efficient, these methods may produce non-positive weights.

In [12], Saye proposes a recursive method that identifies a tangent direction  $e_i$  where  $|\partial_{x_i} F|$  is bounded away from zero on  $\mathcal{U}$ . The implicit function theorem then yields a height function  $h = h(x_1, \dots, x_{i-1}, x_{i+1}, \dots, x_d)$ , representing  $\Gamma \cap \mathcal{U}$  as the graph of  $h$ . Integrating first along the tangent direction produces a recursive formula that achieves high-order accuracy. Similar concepts appear in [2] through specialized “integration directions” that decompose integrals into one-dimensional components,

---

\*Qiu Zhen College, Tsinghua University, Beijing, China (zhaozb21@mails.tsinghua.edu.cn).

and in [1] for domains bounded by two level sets. [10] applies recursion to curvilinear remainders after partitioning regions into tetrahedrobs.

A limitation arises when the required tangent direction does not exist globally. Consider  $\Gamma = \{x^2 + y^2 = 1\} \subset \mathbb{R}^2$ , where neither  $\partial_x F$  nor  $\partial_y F$  maintains uniform sign across the domain. [12] addresses this by subdividing  $U$  into halves processed independently. However, computational constraints necessitate finite subdivision steps, which reduce the Gaussian quadrature order accordingly.

This paper proposes a high-order method that avoids recursion and requires solving only a  $d$ -dimensional linear system at each quadrature node, where  $d$  is the dimension. The domain's geometry is represented using the change of variables formula, and the quadrature rule ensures strictly positive weights.

The focus of this paper is on dimensions  $d = 2$  and  $d = 3$ , and we will mainly focus on the case when  $\Gamma = \{x : F(x) = 0\}$  is compact, and for unclosed surfaces, the vertex displacement algorithm should be treated more carefully. The paper is organized as follows: Sections 2,3,6,7 present the main algorithms, Section 4 discusses mesh adjustment, Section 5 and 8 provides numerical experiments, section 9 summarizes the results.

**2. Quadrature over Curves** We first consider the 2D case to illustrate the main idea. The domain is divided into a triangular mesh,  $U = \cup_{i=1}^N T_i$ , and consequently,

$$\Gamma = \bigcup_{i=1}^N (\Gamma \cap T_i).$$

The integral over  $\Gamma$  is then computed as the sum of integrals over each small piece  $\Gamma \cap T_i$ :

$$\int_{\Gamma} f(\mathbf{x}) dl = \sum_{i=1}^N \int_{\Gamma \cap T_i} f(\mathbf{x}) dl.$$

Without loss of generality, assume  $\Omega = [0, 1]^2$ . The domain can be easily decomposed into a triangular mesh, as shown in Fig. 2.1.

The primary challenge in computing the integral over  $\Gamma \cap T_i$  is the variety of intersection types, as illustrated in Fig. 2.2. To address this, we adjust the triangular mesh to simplify the intersection  $\Gamma \cap T_i$ .

Two mesh adjustment strategies are employed:

1. **Mesh refinement:** Equally divide each rectangle into four smaller rectangles.
2. **Vertex displacement:** Move vertices close to  $\Gamma$  away along the normal direction, as shown in Fig. 2.3.

The vertex displacement is as follows, consider an initial rectangular domain  $[0, 1]^2$  partitioned into  $n^2$  uniform squares, which are further subdivided into  $2n^2$  triangles (see Fig2.3). For a grid point  $(x, y)$  where  $|F(x, y)|$  is sufficiently small, we displace it along the direction  $\text{sgn}(F(x, y)) \cdot \nabla F(x, y)$  by a distance  $ch$ , where  $h$  denotes the mesh size and  $c$  is a tunable parameter (numerical experiments suggest  $c = \frac{1}{4}$ ). Notably, boundary grid points are constrained to prevent movement perpendicular to the boundary. For instance, a left boundary point can only shift vertically, not horizontally. This adjustment ensures that all interior grid points (excluding corners) maintain a sufficient distance from  $\Gamma$ . For smooth  $\Gamma$ , these strategies ensure that the

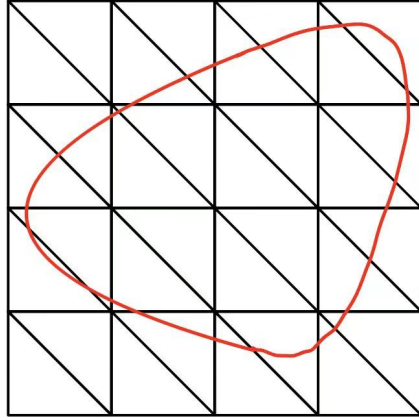


Fig. 2.1: Illustration of domain decomposition.

intersection  $\Gamma \cap T_i$  has only one type, as shown in Fig. 2.2(a). The proof is provided in Section 4.

For smooth  $\Gamma$ , these strategies ensure that the intersection  $\Gamma \cap T_i$  has only one type, as shown in Fig. 2.2(a). The proof is provided in Section 4.

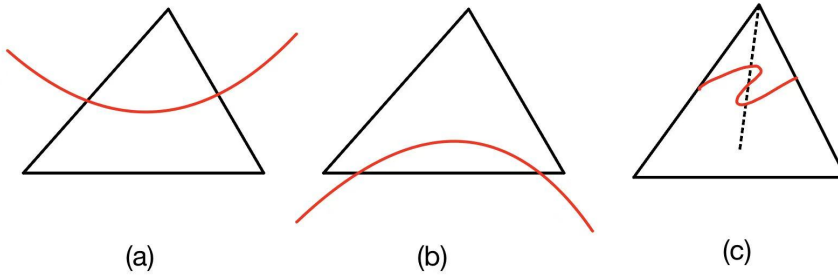


Fig. 2.2: Types of intersections  $\Gamma \cap T_i$ .

For the intersection shown in Fig. 2.2(a), a parametrization of  $\Gamma \cap T_i$  is straightforward, as illustrated in Fig. 2.4, enabling high-accuracy integral computation.

In Fig. 2.4, let  $\gamma \subseteq \mathbb{R}^2$  denote the curve connecting  $B_1$  and  $B_2$ , and let  $\gamma_0$  denote the line segment connecting  $B_1$  and  $B_2$ . The natural parametrization of  $\gamma_0$  is given by  $\phi : [0, 1] \rightarrow \gamma_0$ :

$$\phi(\lambda) = ((1 - \lambda)a_1 + \lambda a_2, \quad (1 - \lambda)b_1 + \lambda b_2).$$

The map  $\Phi : \gamma_0 \rightarrow \gamma$  maps a point  $X$  in  $\gamma_0$  to the intersection point  $Y$  of the line  $AX$  and the curve  $\gamma$ . Under this definition:

$$\int_{\gamma} f(x) ds = \int_0^1 f(\Phi(\phi(t))) (\det(G(\Phi \circ \phi))(t))^{\frac{1}{2}} dt,$$

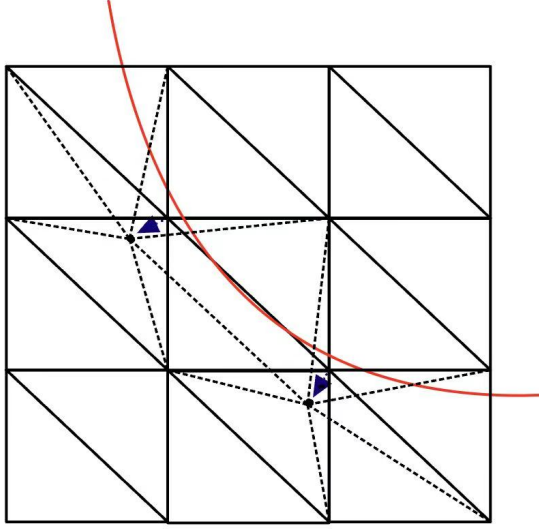


Fig. 2.3: Illustration of mesh adjustment: moving vertices away from  $\Gamma$ .

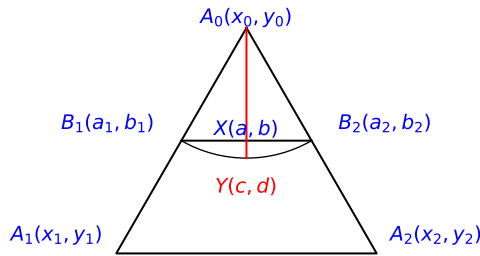


Fig. 2.4: Parametrization of  $\Gamma \cap T_i$ .

where  $G$  is the Gram matrix  $G(g) = J(g)^T J(g)$ , and  $J(g)$  is the Jacobian of  $g$ .

The implicit function relation is derived as follows: Let  $(a, b) = ((1 - \lambda)a_1 + \lambda a_2, (1 - \lambda)b_1 + \lambda b_2)$ . Then:

$$(a - x_0)(d - y_0) - (c - x_0)(b - y_0) = 0,$$

or more precisely:

$$((1 - \lambda)a_1 + \lambda a_2 - x_0)(d - y_0) - (c - x_0)((1 - \lambda)b_1 + \lambda b_2 - y_0) = 0.$$

Additionally, the constraint  $F(c, d) = 0$  must hold. These two conditions define an implicit function relation  $H(\lambda, c, d) = 0$ , where  $H : \mathbb{R}^3 \rightarrow \mathbb{R}^2$  is given by:

$$H(\lambda, c, d) = \begin{pmatrix} F(c, d) \\ ((1 - \lambda)a_1 + \lambda a_2 - x_0)(d - y_0) - (c - x_0)((1 - \lambda)b_1 + \lambda b_2 - y_0) \end{pmatrix}.$$

By the implicit function theorem,  $(c, d)$  can be expressed as a function of  $\lambda$ , which is  $\Phi \circ \phi$ . The Jacobian is:

$$J(\Phi \circ \phi) = - \left( \frac{\partial H}{\partial(c, d)} \right)^{-1} \frac{\partial H}{\partial \lambda}.$$

Since:

$$\frac{\partial H}{\partial(c, d)} = \begin{pmatrix} \frac{\partial F}{\partial x} & \frac{\partial F}{\partial y} \\ (1-\lambda)b_1 + \lambda b_2 - y_0 & (1-\lambda)a_1 + \lambda a_2 - x_0 \end{pmatrix},$$

and:

$$\frac{\partial H}{\partial \lambda} = \begin{pmatrix} 0 \\ (x-x_0)(b_2-b_1) - (y-y_0)(a_2-a_1) \end{pmatrix},$$

the final quadrature rule is obtained as follows: For a given  $\lambda$ , solve  $(c, d)$  via one-dimensional root finding (high-order accurate), and then compute:

$$J(\Phi \circ \phi)(\lambda) = - \begin{pmatrix} \frac{\partial F}{\partial x}(c, d) & \frac{\partial F}{\partial y}(c, d) \\ (1-\lambda)b_1 + \lambda b_2 - y_0 & (1-\lambda)a_1 + \lambda a_2 - x_0 \end{pmatrix}^{-1} \begin{pmatrix} 0 \\ (x-x_0)(b_2-b_1) - (y-y_0)(a_2-a_1) \end{pmatrix}.$$

The integral becomes:

$$\int_{\gamma} f(x) ds = \int_0^1 f(\Phi(\phi(t))) (\det ((J(\Phi \circ \phi)(t))^T J(\Phi \circ \phi)(t)))^{\frac{1}{2}} dt.$$

This integral is computed over a finite interval, allowing the use of standard Gauss-Legendre quadrature for high-order accuracy.

The complete algorithm is summarized in Algorithm 1.

**3. Integration over Hypersurfaces** This section extends the method to 3D. The strategy is similar: divide  $U = [0, 1]^3$  into tetrahedrons,  $U = \cup_{i=1}^N T_i$ , and handle each tetrahedron separately. The tetrahedral mesh is constructed by first decomposing  $U$  into cubes, each of which is divided into five tetrahedrons, as illustrated in Fig. 3.1.

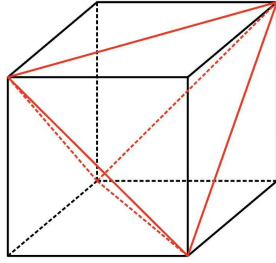


Fig. 3.1: Decomposition of a cube into tetrahedrons.

As in the 2D case, the mesh is adjusted to simplify the intersection  $\Gamma \cap T_i$ . Section 4 proves that the intersection has only two types, as shown in Fig. 3.2.

For Case 2 in Fig.3.2, the tetrahedron  $A_0A_1A_2A_3$  is divided into two sub-tetrahedrons:  $A_0A_1B_2A_3$  and  $A_2A_1B_2A_3$ . Each sub-tetrahedron reduces to Case 1.

---

**Algorithm 1** Line Integral in One Triangle with Node Reordering
 

---

```

1: Input: Vertices  $(x_0, y_0), (x_1, y_1), (x_2, y_2)$ , function  $F$ ,
2:   integrand  $f$ , derivatives  $F_x, F_y$ , quadrature order  $q$ .
3: Output: Integral value  $I$ .
4: if  $F(x_0, y_0)F(x_1, y_1) > 0$  and  $F(x_0, y_0)F(x_2, y_2) > 0$  then
5:   return 0
6: else if  $F(x_0, y_0)F(x_1, y_1) > 0$  and  $F(x_0, y_0)F(x_2, y_2) < 0$  then
7:   Swap  $(x_0, y_0)$  with  $(x_2, y_2)$ 
8: else if  $F(x_0, y_0)F(x_1, y_1) < 0$  and  $F(x_0, y_0)F(x_2, y_2) > 0$  then
9:   Swap  $(x_0, y_0)$  with  $(x_1, y_1)$ 
10: end if
11:  $(a_1, b_1) \leftarrow$  Intersection of line  $(x_0, y_0)-(x_1, y_1)$  with  $\{F = 0\}$ 
12:  $(a_2, b_2) \leftarrow$  Intersection of line  $(x_0, y_0)-(x_2, y_2)$  with  $\{F = 0\}$ 
13: Let  $\lambda_1, \lambda_2, \dots, \lambda_q$  be Gauss-Legendre nodes on  $[0, 1]$ 
14: Let  $\omega_1, \omega_2, \dots, \omega_q$  be corresponding weights
15: Initialize  $I \leftarrow 0$ 
16: for  $i = 1$  to  $q$  do
17:    $(a, b) \leftarrow ((1 - \lambda_i)a_1 + \lambda_i a_2, (1 - \lambda_i)b_1 + \lambda_i b_2)$ 
18:    $(c, d) \leftarrow$  Intersection of line  $(x_0, y_0)-(a, b)$  with  $\{F = 0\}$ 
19:   Compute Jacobian  $J$  for point  $(c, d)$ :
20:     
$$J = \begin{pmatrix} F_x(c, d) & F_y(c, d) \\ b - y_0 & a - x_0 \end{pmatrix}^{-1} \begin{pmatrix} 0 \\ (x - x_0)(b_2 - b_1) - (y - y_0)(a_2 - a_1) \end{pmatrix}$$

21:    $I \leftarrow I + \omega_i \cdot f(c, d) \cdot \sqrt{J^T J} \cdot ds$ 
22: end for
23: return  $I$ 

```

---

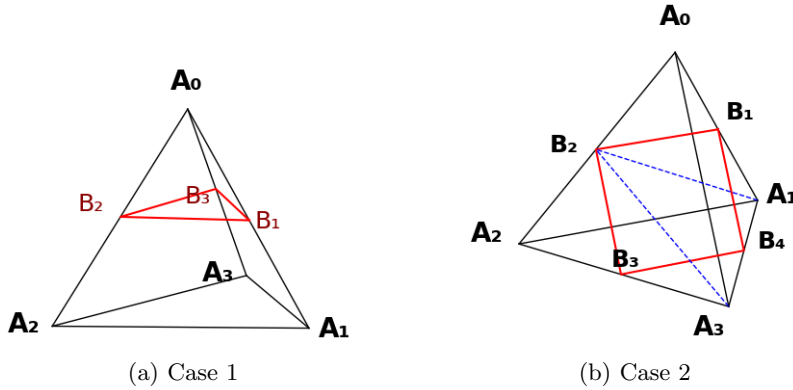


Fig. 3.2: Types of intersections  $\Gamma \cap T_i$  in 3D.

The method for computing the integral in Case 1 is as follows. First, parametrize the intersection  $\Gamma \cap T_i$ , as shown in Fig. 3.3.

Let  $S_0$  denote the triangle  $B_1B_2B_3$ , and  $\Gamma_0$  denote the intersection of the hyper-surface with the tetrahedron. The triangle has a natural parametrization:

$$\{(\mu_1, \mu_2) : \mu_1, \mu_2 \in [0, 1], \mu_1 + \mu_2 \leq 1\} \rightarrow S_0,$$

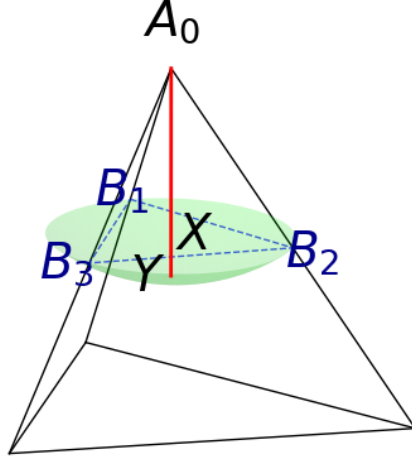


Fig. 3.3: Parametrization of  $\Gamma \cap T_i$  in 3D.

given by:

$$(\mu_1, \mu_2) \rightarrow ((1 - \mu_1 - \mu_2)a_3 + \mu_1 a_1 + \mu_2 a_2, (1 - \mu_1 - \mu_2)b_3 + \mu_1 b_1 + \mu_2 b_2, (1 - \mu_1 - \mu_2)c_3 + \mu_1 c_1 + \mu_2 c_2).$$

The map from  $S_0$  to  $\Gamma_0$  projects a point  $X$  in  $S_0$  to the intersection point  $Y = \overline{A_0 X} \cap \Gamma_0$ . The implicit function relation between  $\mu_1, \mu_2, x, y, z$  is given by  $\Phi(\mu_1, \mu_2, x, y, z) = 0$ , where  $\Phi : \mathbb{R}^5 \rightarrow \mathbb{R}^3$  is defined as:

$$\Phi(\mu_1, \mu_2, x, y, z) = \begin{pmatrix} F(x, y, z) \\ (x - x_0)(b - y_0) - (y - y_0)(a - x_0) \\ (x - x_0)(c - z_0) - (z - z_0)(a - x_0) \end{pmatrix},$$

with:

$$(a, b, c) = ((1 - \mu_1 - \mu_2)a_3 + \mu_1 a_1 + \mu_2 a_2, (1 - \mu_1 - \mu_2)b_3 + \mu_1 b_1 + \mu_2 b_2, (1 - \mu_1 - \mu_2)c_3 + \mu_1 c_1 + \mu_2 c_2).$$

By the implicit function theorem,  $(x, y, z)$  can be expressed as a function of  $(\mu_1, \mu_2)$ , denoted  $(x(\boldsymbol{\mu}), y(\boldsymbol{\mu}), z(\boldsymbol{\mu}))$ . The Jacobian is:

$$J = - \left( \frac{\partial \Phi}{\partial \mathbf{x}} \right)^{-1} \frac{\partial \Phi}{\partial \boldsymbol{\mu}}.$$

Explicitly:

$$\frac{\partial \Phi}{\partial \mathbf{x}} = \begin{pmatrix} \frac{\partial F}{\partial x} & \frac{\partial F}{\partial y} & \frac{\partial F}{\partial z} \\ b - y_0 & x_0 - a & 0 \\ c - z_0 & 0 & x_0 - a \end{pmatrix},$$

$$\frac{\partial \Phi}{\partial \boldsymbol{\mu}} = \begin{pmatrix} 0 & 0 \\ (x - x_0)(b_1 - b_3) - (y - y_0)(a_1 - a_3) & (x - x_0)(b_2 - b_3) - (y - y_0)(a_2 - a_3) \\ (x - x_0)(c_1 - c_3) - (z - z_0)(a_1 - a_3) & (x - x_0)(c_2 - c_3) - (z - z_0)(a_2 - a_3) \end{pmatrix}.$$

The integral is transformed to  $S_0$ :

$$\int_{\Gamma_0} f(x) ds = \int_{S_0} f(x(\boldsymbol{\mu}), y(\boldsymbol{\mu}), z(\boldsymbol{\mu})) \sqrt{\det(J^T J)} d\boldsymbol{\mu}.$$

A final change of variables maps  $S_0$  to  $[0, 1]^2$ :

$$\mu_1 = u, \quad \mu_2 = (1 - u)v, \quad (u, v) \in [0, 1]^2.$$

This reduces the integral over  $\Gamma \cap T_i$  to an integral over  $[0, 1]^2$ , which is computed using standard Gauss-Legendre quadrature for high precision.

#### 4. Analysis of Mesh Adjustment

DEFINITION 4.1. *Let  $M \subset \mathbb{R}^3$  be a smooth submanifold. The **reach** of  $M$ , denoted  $r_M$ , is the largest value such that for any point  $x \in \mathbb{R}^3$  with  $d(x, M) \leq r_M$ , the projection  $\pi_M(x)$  is unique. That is, there exists a unique  $y \in M$  such that  $d(x, y) = d(x, M)$ .*

The following proposition is proved in [4]:

PROPOSITION 4.1. *For a compact smooth submanifold  $M \subset \mathbb{R}^3$ , the reach  $r_M > 0$ .*

Let  $\Gamma = \{x \in \mathbb{R}^3 : F(x) = 0\}$  be a smooth compact surface, with  $\kappa_1(x), \kappa_2(x)$  denoting the principal curvatures at  $x \in \Gamma$ . Define:

$$K_\Gamma = \frac{1}{2} \max_{x \in \Gamma} (|\kappa_1(x)| + |\kappa_2(x)|).$$

Let  $T = \cup_{i=1}^N T_i$  be a tetrahedral mesh, where each  $T_i$  is a tetrahedron. Let:

$$h_T = \max_{i=1, \dots, N} \text{diam}(T_i).$$

DEFINITION 4.2. *A mesh  $T$  is  $\eta$ -consistent with  $\Gamma$  if:*

- $h_T \leq r_\Gamma$ , where  $r_\Gamma$  is the reach of  $\Gamma$ .
- $\text{dist}(V_T, \Gamma) \geq \eta h_T$ , where  $V_T$  is the set of all vertices of  $T$ .

The main theorem is stated as follows:

THEOREM 4.1. *Let  $\Gamma = \{x \in \mathbb{R}^3 : F(x) = 0\}$  be a smooth compact surface, and  $T$  a tetrahedral mesh. If  $T$  is  $\eta$ -consistent with  $\Gamma$  and  $\eta > K_\Gamma h_T$ , then for each tetrahedron  $T_i = A_0 A_1 A_2 A_3$ , the intersection  $\Gamma \cap T_i$  has only three possible forms:*

- (1) *If  $F(A_i)$  has the same sign for all  $i = 0, 1, 2, 3$ , then  $\Gamma \cap T_i = \emptyset$ .*
- (2) *If  $F(A_0) > 0 (< 0)$  and  $F(A_1), F(A_2), F(A_3) < 0 (> 0)$ , then for any  $P \in \Delta A_1 A_2 A_3$ , the line segment  $\overline{A_0 P}$  intersects  $\Gamma$  exactly once.*
- (3) *If  $F(A_0), F(A_1) > 0 (< 0)$  and  $F(A_2), F(A_3) < 0 (> 0)$ , then  $\overline{A_0 A_2}$  intersects  $\Gamma$  exactly once at  $B$ , and for any  $P \in \Delta B A_1 A_3$ , the segments  $\overline{A_0 P}$  and  $\overline{A_2 P}$  intersect  $\Gamma$  exactly once.*

The proof relies on the following lemma:

LEMMA 4.1. *Under the assumptions of Theorem 4.1, for any tetrahedron  $T_i = A_0 A_1 A_2 A_3$  and any point  $B \in \Delta A_1 A_2 A_3$ , the line segment  $A_0 B$  intersects  $\Gamma$  at most once.*

*Proof.* [Proof of Theorem 4.1] If all  $F(A_i)$  share the same sign, suppose  $\Gamma$  intersects the tetrahedron. By Lemma 4.1, any edge  $A_i A_j$  intersects  $\Gamma$  at most once. However, the Intermediate Value Theorem requires a sign change on intersecting edges, contradicting uniform signs. Hence, no intersection exists.

For Case 2, for  $P \in \Delta A_1 A_2 A_3$ , the segment  $\overline{A_0 P}$  connects  $A_0$  (opposite sign) and  $P$  (same sign as  $A_1$ ). The Intermediate Value Theorem ensures an intersection, and Lemma 4.1 guarantees uniqueness.

For Case 3, the edge  $\overline{A_0A_2}$  intersects  $\Gamma$  exactly once at  $B$  due to the sign change and Lemma 4.1. For  $P \in \triangle BA_1A_3$ , segments  $\overline{A_0P}$  and  $\overline{A_2P}$  cross  $\Gamma$  due to sign differences, with uniqueness ensured by Lemma 4.1.  $\square$

Lemma 4.1 follows from Lemma 4.2:

LEMMA 4.2. *Let  $d(x, \Gamma)$  be the signed distance function for  $\Gamma$ . For any  $A, B \in \mathbb{R}^3$  with  $h = \|A - B\| < r_\Gamma$  and  $hK_\Gamma \leq 1/4$ , if the line segment  $AB$  intersects  $\Gamma$  twice, then:*

$$\max\{d(A, \Gamma), d(B, \Gamma)\} \leq K_\Gamma h^2.$$

*Proof.* Let  $x(t) = A + t(B - A)/h$  and  $d(t) = d(x(t), \Gamma)$ . We first show  $d(t) \in C^1[0, h]$ .

Using the implicit function theorem, let  $\mathbf{y} = \pi_\Gamma(x)$  be the closest point projection of  $\mathbf{x}$ . The implicit relation  $G(t, \mathbf{y}, \xi) = 0$  is defined as:

$$G(t, \mathbf{y}, \xi) = \begin{pmatrix} F(\mathbf{y}) \\ \mathbf{x}(t) - \mathbf{y} - \xi \nabla F(\mathbf{y}) \end{pmatrix}.$$

The Jacobian  $\frac{\partial G}{\partial(\mathbf{y}, \xi)}$  is invertible under the smoothness of  $F$  and small  $\xi$ , ensuring  $d(t)$  is smooth.

Let  $\mathbf{v} = (B - A)/\|B - A\|$  and  $\mathbf{n}(\mathbf{y})$  denote the outer normal of  $\Gamma$  at  $\mathbf{y}$ . The projection satisfies:

$$\mathbf{x}(t) = \pi(\mathbf{x}(t)) + d(t)\mathbf{n}(\pi(\mathbf{x}(t))).$$

Differentiating with respect to  $t$  yields:

$$\mathbf{v} = \frac{d\pi}{dt} + d'(t)\mathbf{n} + d(t)\frac{d\mathbf{n}}{dt}.$$

Since  $\frac{d\pi}{dt} \cdot \mathbf{n} = 0$  and  $\frac{d\mathbf{n}}{dt} \cdot \mathbf{n} = 0$ , we have:

$$d'(t) = \mathbf{v} \cdot \mathbf{n}(\pi(\mathbf{x}(t))), \quad \mathbf{v}_{\text{tan}} = (I - d(t)S)\frac{d\pi}{dt},$$

where  $\mathbf{v}_{\text{tan}} = \mathbf{v} - (\mathbf{v} \cdot \mathbf{n})\mathbf{n}$ , and  $S$  is the Weingarten map with principal curvatures  $\kappa_1, \kappa_2$  and eigenvectors  $\mathbf{e}_1, \mathbf{e}_2$ .

The second derivative is:

$$d''(t) = -\mathbf{v} \cdot S(I - d(t)S)^{-1}\mathbf{v}_{\text{tan}} = -\sum_{i=1}^2 \frac{\kappa_i v_i^2}{1 - d(t)\kappa_i},$$

where  $v_i = \mathbf{v} \cdot \mathbf{e}_i$ . Since  $|d(t)| \leq h$  and  $|d(t)\kappa_i| \leq 2hK_\Gamma \leq 1/2$ , we have:

$$|d''(t)| \leq \sum_{i=1}^2 \left| \frac{\kappa_i v_i^2}{1 - d(t)\kappa_i} \right| \leq 2K_\Gamma.$$

If  $AB$  intersects  $\Gamma$  twice at  $t_1, t_2 \in [0, h]$ , the error of Lagrange interpolation gives:

$$|d(t)| \leq \frac{1}{2} \left( \max_{t \in [0, h]} |d''(t)| \right) |(t - t_1)(t - t_2)|,$$

which implies:

$$\max\{d(A, \Gamma), d(B, \Gamma)\} = \max\{d(0), d(h)\} \leq K_\Gamma h^2.$$

□

Then we consider the following adjust algorithm: For a grid point  $x$ , let  $n \geq 2$  to be determined, if  $|F(x)| \leq \frac{Mh}{n}$ , then move it along  $\text{sgn}(F(x)) \cdot \nabla F(x)$  direction, for length  $\frac{h}{n}$ . Recall that we assume  $h \leq r$  where  $r$  is the reach of  $\Gamma$ .

LEMMA 4.3. *Under the above adjustment, when  $h$  is sufficiently small that satisfies  $\forall y \in B(x, h)$ ,  $\left| \left( \frac{\nabla F(x)}{\|\nabla F(x)\|} - \frac{\nabla F(y)}{\|\nabla F(y)\|} \right) \right| \leq \frac{1}{2}$ , then for every node  $A$ , we have  $d(A, \Gamma) \geq \frac{h}{2n}$*

*Proof.* For any point  $x$ , let  $x_1$ , be the point under the above adjustment.

- (1) If  $d(x, \Gamma) \geq \frac{h}{2}$ . then  $d(x_1, \Gamma) \geq \frac{h}{2} - \frac{h}{n} > \frac{h}{2n}$
- (2) If  $d(x, \Gamma) < \frac{h}{2}$ . let  $x_2$  lies on the ray  $\overline{yx}$ , with  $d(x, x_2) = \frac{h}{n}$ . since  $d(x_2, \Gamma) < h \leq r$ , and  $r$  is the reach of  $\Gamma$ , we have  $d(x_2, \Gamma) = d(x_2, y) \geq \frac{h}{n}$  and then

$$\begin{aligned} d(x_1, x_2) &= \frac{h}{n} \left| \left( \frac{\nabla F(x)}{\|\nabla F(x)\|} - \frac{\nabla F(y)}{\|\nabla F(y)\|} \right) \right| \\ &\leq \frac{h}{2n} \end{aligned}$$

(when  $h$  sufficiently small). Hence we have

$$d(x_1, \Gamma) \geq \frac{h}{2n}$$

in both cases. □

In summary, we have proved that, under the adjustment of triangulations, the intersection of the curve(surface) and the triangle(tetrahedron) can only be the ways shown in figure 1 and figure 5(a). We summary it as the following theorem:

THEOREM 4.2. *For a point  $X$ , if  $h$  sufficiently small and  $n \geq 2$  that satisfies:*

- (1)  $\forall y \in B(x, h)$ ,  $\left| \left( \frac{\nabla F(x)}{\|\nabla F(x)\|} - \frac{\nabla F(y)}{\|\nabla F(y)\|} \right) \right| \leq \frac{1}{2}$
- (2)  $h\kappa_i \leq \frac{1}{2}$ ,  $i = 1, 2$  holds for all  $y \in B(x, h)$ .
- (3)  $h \leq \frac{1}{2n(\kappa_1 + \kappa_2)}$ ,  $\forall y \in B(x, h)$ .
- (4)  $h \leq r$  where  $r$  is the reach of  $\Gamma$ .

*Then under the algorithm that moves  $x$  along  $\text{sgn}(F(x)) \cdot \nabla F(x)$  direction, for length  $\frac{h}{n}$  when  $|F(x)| \leq \frac{M(h)h}{n}$ , all tetrahedrons intersects with  $\Gamma$  by the way stated in theorem 4.1.*

**5. Numerical tests for line and surface integrals** In this section we show some numerical tests, include integration on curves and surfaces.

**Test 1: Ellipse**  $F(x, y) = x^2 + 4y^2 - 1$ ,  $f(x, y) = x^2$ . The error is plotted in Fig. 5.1.

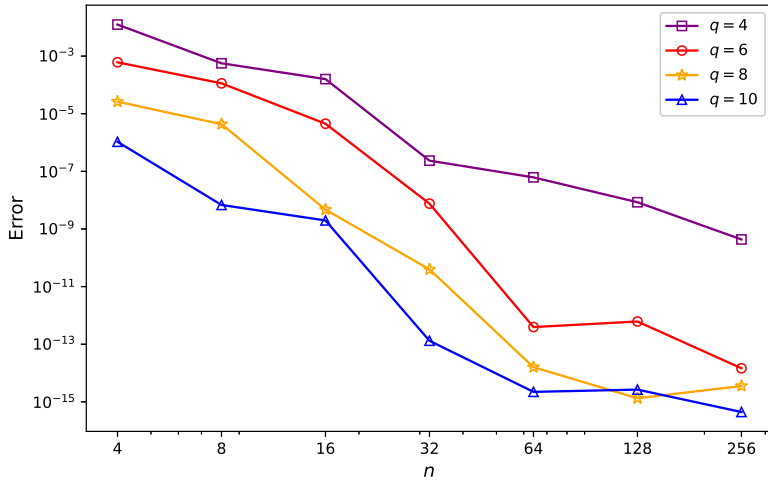


Fig. 5.1: Error in Test 1.  $q$ : order of Gauss-Legendre quadrature.

From Fig.5.1, we see the order increases as  $q$  increases. Note that the machine precision is approximately  $10^{-16}$ , which means that the error when  $n=256$  is sufficiently small.

**Test 2: Non-closed and non-polynomial curve**  $F(x, y) = y - e^x$ ,  $x \in [0, 1]$ .  $f(x, y) = \sqrt{1 + e^{2x}}$ . The integral can be solved explicitly and the result is  $\frac{e^2+1}{2}$ . The result is given in Fig. 5.2.

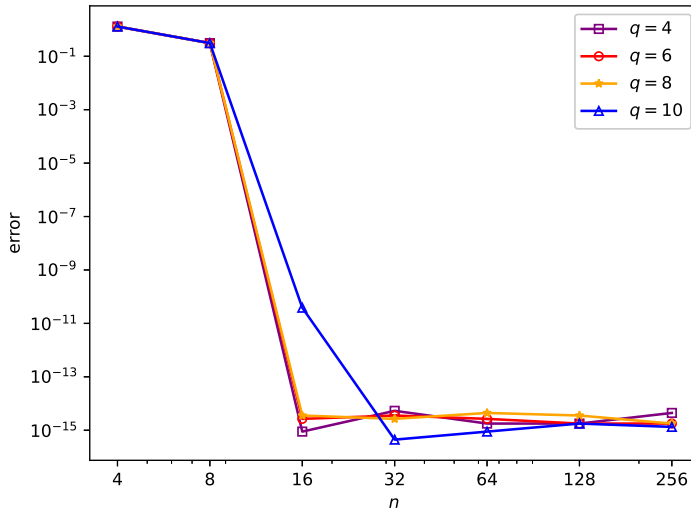


Fig. 5.2: Error in Test 2.  $q$ : order of Gauss-Legendre quadrature.

**Test 3: Surface area of ellipsoid** Consider the surface  $\Gamma \in \mathbb{R}^3$  given by

$x^2 + 4y^2 + 9z^2 = 0$ . We use our algorithm, choose  $q = 6, 8, 10, 12$  and plot the error in Fig. 5.3.

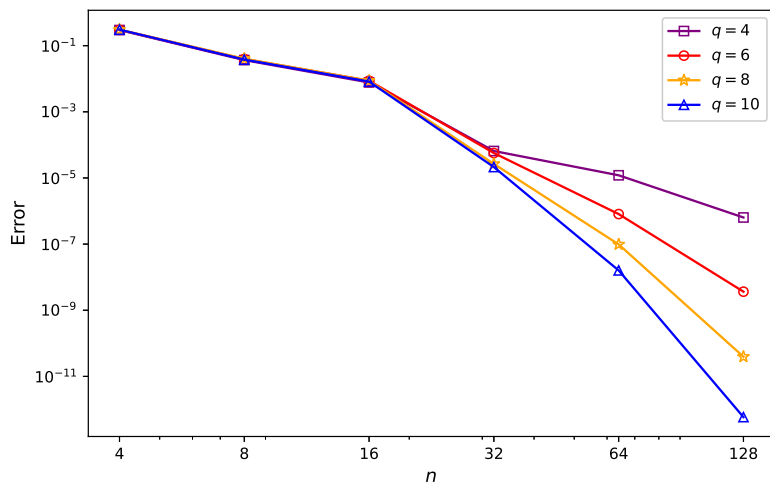


Fig. 5.3: Error in Test 3.  $q$ : order of Gauss-Legendre quadrature.

The scheme is indeed high order, and when  $q = 12$ ,  $n = 128$ , the error is almost machine precision.

**Test 4: Integral on a nonclosed surface with non-trivial integrand**

Consider the surface  $\Gamma \in \mathbb{R}^3$  given by  $x^2 + y^2 - z^2 = 0$ , where  $(x, y) \in [-1, 1]^2$ . Let  $f(x, y, z) = \sqrt{1 + 4x^2 + 4y^2}$ , then the exact integral can be computed via change of variables:

$$\int_{\Gamma} f ds = \int_{[-1,1]^2} (1 + 4x^2 + 4y^2) dx dy = \frac{44}{3}$$

we use our algorithm, choose  $q = 4, 6, 8, 10$  and plot the error, see Fig. 5.4.

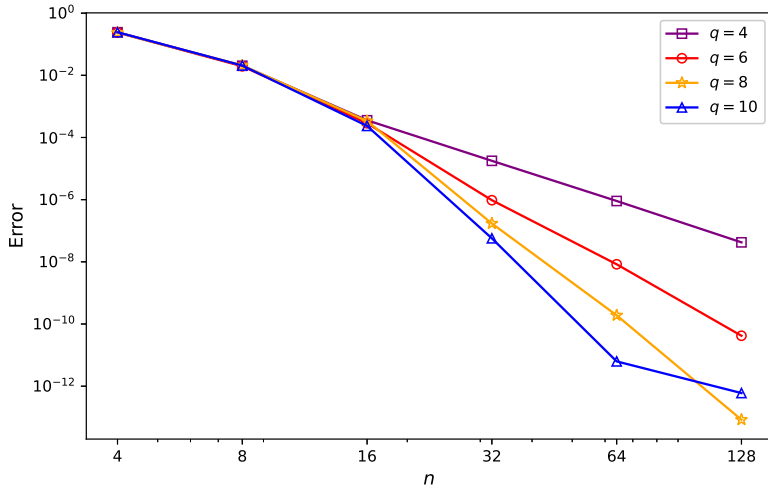


Fig. 5.4: Error in Test 4.  $q$ : order of Gauss-Legendre quadrature.

**6. Integration over 2d region** In this section we consider the integration over a region  $\Omega := \{F \leq 0\}$ .

The idea is similar with Section 3, we first divide the whole domain into triangles as

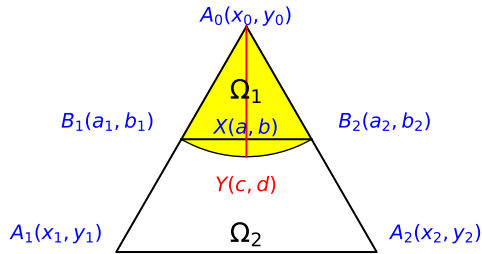


Fig. 6.1: Illustration of the parametrization of the 2D region

in Figure 2.1, and then adjust the nodes as in Figure 2.3 to ensure that the intersection  $\Gamma \cap T_i$  has only one type shown in Figure 2.2(a).

Now suppose  $U = \cup_{i=1}^N T_i$ , then we have:

$$\Omega = \bigcup_{i=1}^N (\Omega \cap T_i).$$

The integral over  $\Omega$  is then computed as the sum of integrals over each small piece

$\Omega \cap T_i$ :

$$\int_{\Omega} f(\mathbf{x}) d\mathbf{x} = \sum_{i=1}^N \int_{\Omega \cap T_i} f(\mathbf{x}) d\mathbf{x}.$$

Consider each triangle  $T_i$ , the intersection  $\Omega \cap T_i$  can be either  $\Omega_1$  or  $\Omega_2$  in Figure 6.1. Since standard Gauss-Legendre quadrature rule can be applied to  $T_i$ , so we have

$$\int_{\Omega_2} f(\mathbf{x}) d\mathbf{x} = \int_{T_i} f(\mathbf{x}) d\mathbf{x} - \int_{\Omega_1} f(\mathbf{x}) d\mathbf{x}$$

Hence we only consider the quadrature on  $\Omega_1$ .

As shown in Figure 6.1, the parameterization from the triangle  $A_0B_1B_2$  to the region  $\Omega_1$  is defined as follows: for any point  $X \in B_1B_2$ , let  $Y$  be the intersection of  $A_0X$  and  $\{F = 0\}$ , we stretch the line segment  $A_0X$  uniformly to  $A_0Y$ . More precisely, let  $(x_0, y_0)$ ,  $(a_1, b_1)$ ,  $(a_2, b_2)$  be the vertices of triangle  $A_0B_1B_2$  and  $\vec{v}_0 = (x_0, y_0)$ ,  $\vec{v}_1 = (a_1 - x_0, b_1 - y_0)$ ,  $\vec{v}_2 = (a_2 - a_1, b_2 - b_1)$ , then the triangle can be parameterized by

$$\vec{v} = \vec{v}_0 + \lambda_1 \vec{v}_1 + \lambda_2 \vec{v}_2 \quad \lambda_1, \lambda_2 \in [0, 1] \quad \lambda_1 \geq \lambda_2$$

The transformation  $a = \lambda_1$ ,  $b = \frac{\lambda_2}{\lambda_1}$ ,  $a, b \in [0, 1]^2$  gives us another parametrization.

In section 2 we have defined a map with known Jacobian

$$H : b \in [0, 1] \rightarrow \mathbb{R}^2$$

via figure 2.4. denote it as  $H(b) = (h_1(b), h_2(b))$ . Then we have our parametrization:

$$\begin{aligned} G : [0, 1]^2 &\rightarrow \Omega_1 \\ (a, b) &\longrightarrow (1 - a)\vec{V}_0 + aH(b) \end{aligned}$$

with Jacobian matrix

$$J(G) = \begin{pmatrix} h_1(b) - x_0 & ah'_1(b) \\ h_2(b) - y_0 & ah'_2(b) \end{pmatrix}$$

By change of variable formula, we have

$$\int_{\Omega_1} f = \int_{[0,1]^2} \det J(G) \cdot f(G(a, b)) da db$$

Standard Gauss-Legendre quadrature rule can be applied to compute the integral.

The whole calculation can be summarized as Algorithm 2.

**7. Integration over 3d region** In this section we consider the integration over a region  $\Omega \subseteq \mathbb{R}^3$  defined by  $\{F \leq 0\}$ .

The strategy is similar: divide  $\Omega = [0, 1]^3$  into tetrahedrons,  $\Omega = \cup_{i=1}^N T_i$ , and handle each tetrahedron separately. As in the 2D case, the mesh is adjusted to simplify the intersection  $\Gamma \cap T_i$ . Section 4 proves that the intersection has only two types, as

---

**Algorithm 2** Region Integral in One Triangle with Changing the Order

---

1: **Input:** Vertices  $(x_0, y_0), (x_1, y_1), (x_2, y_2)$ , function  $F$ , integrand  $f$ , derivatives  $F_x, F_y$ , quadrature order  $q$ . The region of integration is the intersection of  $\{F < 0\}$  and the triangle.

2: **Output:** Integral value  $I$ .

3: Set  $I_0$  to be the integral of  $f$  over the whole triangle, computed by Gauss-Legendre quadrature rule.

4: **if**  $F(x_0, y_0)F(x_1, y_1) > 0$  **and**  $F(x_0, y_0)F(x_2, y_2) > 0$  **and**  $F(x_0, y_0) > 0$  **then**

5:     **return** 0

6: **else if**  $F(x_0, y_0)F(x_1, y_1) > 0$  **and**  $F(x_0, y_0)F(x_2, y_2) > 0$  **and**  $F(x_0, y_0) < 0$  **then**

7:     **return**  $I_0$

8: **else if**  $F(x_0, y_0)F(x_1, y_1) > 0$  **and**  $F(x_0, y_0)F(x_2, y_2) < 0$  **then**

9:     Swap  $(x_0, y_0)$  with  $(x_2, y_2)$

10: **else if**  $F(x_0, y_0)F(x_1, y_1) < 0$  **and**  $F(x_0, y_0)F(x_2, y_2) > 0$  **then**

11:     Swap  $(x_0, y_0)$  with  $(x_1, y_1)$

12: **end if**

13:  $(a_1, b_1) \leftarrow$  Intersection of line  $(x_0, y_0)-(x_1, y_1)$  with  $\{F = 0\}$

14:  $(a_2, b_2) \leftarrow$  Intersection of line  $(x_0, y_0)-(x_2, y_2)$  with  $\{F = 0\}$

15: Let  $\lambda_1, \lambda_2, \dots, \lambda_q$  be Gauss-Legendre nodes on  $[0, 1]$

16: Let  $\omega_1, \omega_2, \dots, \omega_q$  be corresponding weights

17: Initialize  $I \leftarrow 0$

18: **for**  $i = 1$  **to**  $q$  **do**

19:      $(a, b) \leftarrow ((1 - \lambda_i)a_1 + \lambda_i a_2, (1 - \lambda_i)b_1 + \lambda_i b_2)$

20:      $(c, d) \leftarrow$  Intersection of line  $(x_0, y_0)-(a, b)$  with  $\{F = 0\}$

21:     **for**  $j = 1$  **to**  $q$  **do**

22:          $e \leftarrow (1 - \lambda_j)x_0 + \lambda_j c$

23:          $f \leftarrow (1 - \lambda_j)y_0 + \lambda_j d$

24:         Compute Jacobian:

25:

$$\begin{pmatrix} J_1 \\ J_2 \end{pmatrix} = - \begin{pmatrix} \frac{\partial F}{\partial x} & \frac{\partial F}{\partial y} \\ (1 - \lambda)b_1 + \lambda b_2 - y_0 & (1 - \lambda)a_1 + \lambda a_2 - x_0 \end{pmatrix}^{-1} \begin{pmatrix} 0 \\ (x - x_0)(b_2 - b_1) - (y - y_0)(a_2 - a_1) \end{pmatrix}$$

26:

$$J = \begin{pmatrix} c - x_0 & \lambda_j J_1 \\ d - y_0 & \lambda_j J_2 \end{pmatrix}$$

27:     Update integral:

$$I \leftarrow I + \omega_i f(e, f) |\det(J)|$$

28:     **end for**

29: **end for**

30: **if**  $F(x_0, y_0) > 0$  **then**

31:      $I \leftarrow I_0 - I$

32: **end if**

33: **return**  $I$

---

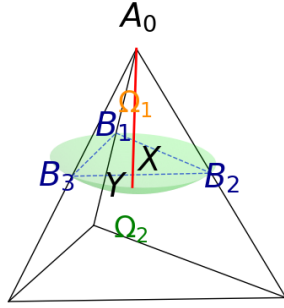


Fig. 7.1: Parametrization of  $\Omega_1$  in 3D.

shown in Fig. 3.2. When case 2 occurs, we divide the region into two tetrahedrons  $B_2A_2A_1A_3$  and  $B_2A_0A_1A_3$  and treat them separately. So we only consider case 1. As shown in figure 7.1, since standard Gauss-Legendre quadrature rule can be applied to the whole tetrahedron, we only need to consider integration on  $\Omega_1$ .

We first introduce some notations. In figure 7.1, let  $(x_0, y_0, z_0)$ ,  $(a_1, b_1, c_1)$ ,  $(a_2, b_2, c_2)$ ,  $(a_3, b_3, c_3)$  be the vertices of the tetrahedron  $A_0B_1B_2B_3$ , and  $\vec{v}_0 = (x_0, y_0, z_0)$ ,  $\vec{v}_1 = (a_1 - a_3, b_1 - b_3, c_1 - c_3)$ ,  $\vec{v}_2 = (a_2 - a_3, b_2 - b_3, c_2 - c_3)$ ,  $\vec{v}_3 = (x_3 - x_0, y_3 - y_0, z_3 - z_0)$ .

Denote  $\Gamma_0$  be the triangle  $(x_1, y_1, z_1)$ ,  $(x_2, y_2, z_2)$ ,  $(x_3, y_3, z_3)$ ,  $\Gamma$  be the zero level-set of  $F$ . The parameterization is similar as the 2d case, for each point  $X \in \Gamma_0$ , denote  $Y$  be the intersection of  $A_0X$  and  $\Gamma$ . We stretch each red line  $A_0X$  in figure 7.1 uniformly to  $A_0Y$  and get the parameterization from the tetrahedron  $A_0B_1B_2B_3$  to  $\Omega_1$ . We use the following parameterization of the tetrahedron  $A_0B_1B_2B_3$

$$\vec{v} = \vec{v}_0 + a\vec{v}_3 + ab\vec{v}_1 + ac\vec{v}_2$$

Where  $a \in [0, 1]$  and  $b, c \in [0, 1]^2$ ,  $b + c \leq 1$ . Define  $T$  to be the region  $\{b, c \in [0, 1]^2, b + c \leq 1\}$ , then  $(a, b, c) \in [0, 1] \times T$ .

In section 3 we have defined a map  $P : T \rightarrow \mathbb{R}^3$  by mapping a point  $x \in \Gamma_0$  into the point  $y = P(x) \in \Gamma$  to be the intersection of  $A_0X$  and  $\Gamma$ . The Jacobian of  $P$  is computed in section 3. Denote  $P(b, c) = (x(b, c), y(b, c), z(b, c))$ .

The parameterization of  $\Omega_1$  is defined as follows: define  $Q : [0, 1] \times T \rightarrow \Omega_1$  by

$$Q(a, b, c) = (1 - a)\vec{x}_0 + aP(b, c)$$

With Jacobian

$$J(Q) = \begin{pmatrix} x(b, c) - x_0 & ax_b & ax_c \\ y(b, c) - y_0 & ay_b & ay_c \\ z(b, c) - z_0 & az_b & az_c \end{pmatrix}$$

where the partial derivatives have been computed in section 3. By change of variables formula,

$$\int_{\Omega_1} f = \int_{[0, 1] \times T} \det J(Q) \cdot f(Q(a, b, c)) da db dc$$

Standard Gauss-Legendre quadrature rule can be applied to compute the integral.

**8. Numerical tests for region integrals** In this section we show some numerical results for region integral.

**Test 1: Area of an ellipse.** Here  $F(x, y) = x^2 + 4y^2 - 1$ , and  $F(x, y) = 0$  is an ellipse,  $f(x, y) = 1$ . The exact result is  $\frac{\pi}{2}$ , we use our method, with  $q = 4, 6, 8, 10$ , to solve the integral. The error is plotted in figure 8.1 as follows:

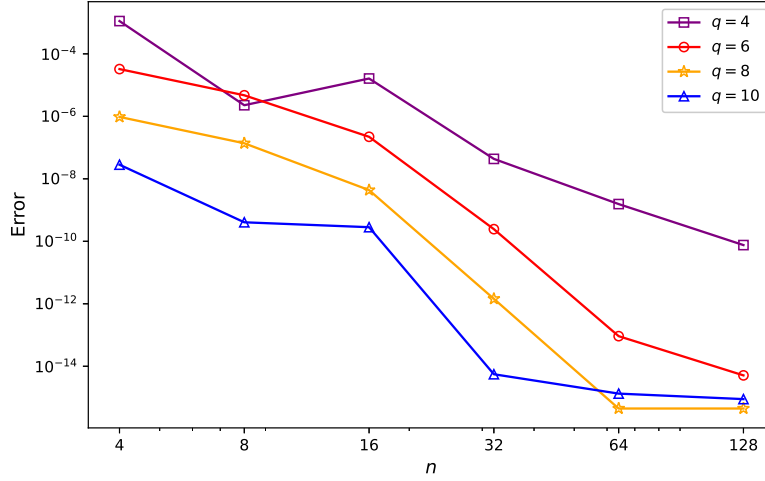


Fig. 8.1: Error of different order q

**Test 2: Area of a region above  $y = x^4$ .** Consider the region  $[-2, 2]^2$  intersect with  $\{y > x^4\}$ , here we choose  $F(x, y) = x^4 - y$  and  $f(x, y) = 1$ . The exact result is  $\frac{8}{5}2^{\frac{5}{4}}$ . We use our method, with  $q = 4, 6, 8, 10$ , to solve the integral. The error is plotted in figure 8.2 as follows:

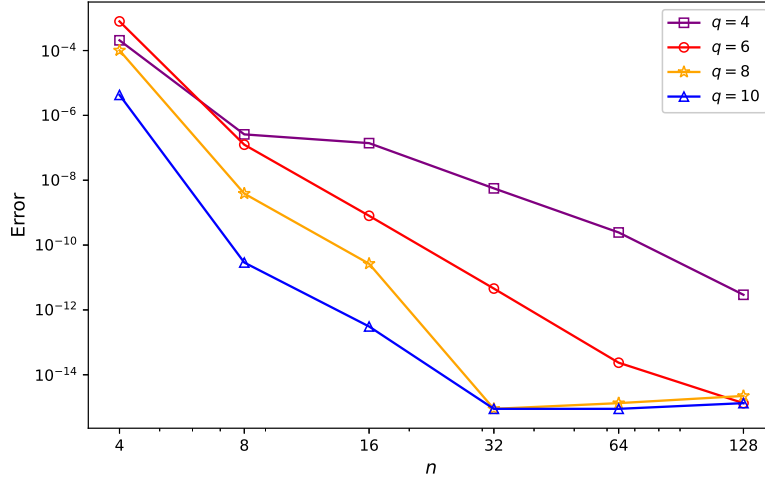


Fig. 8.2: Error of different order q

**Test 3: Volume of an ellipsoid.** Here  $F(x, y) = x^2 + y^2 + 4z^2 - 1$ , and  $F(x, y, z) = 0$  is an ellipsoid.  $f(x, y, z) = 1$ . The exact result is  $\frac{2\pi}{3}$ , and we use our method, with  $q = 4, 6, 8, 10$ , to solve the integral. The error is plotted in figure 8.3 as follows:

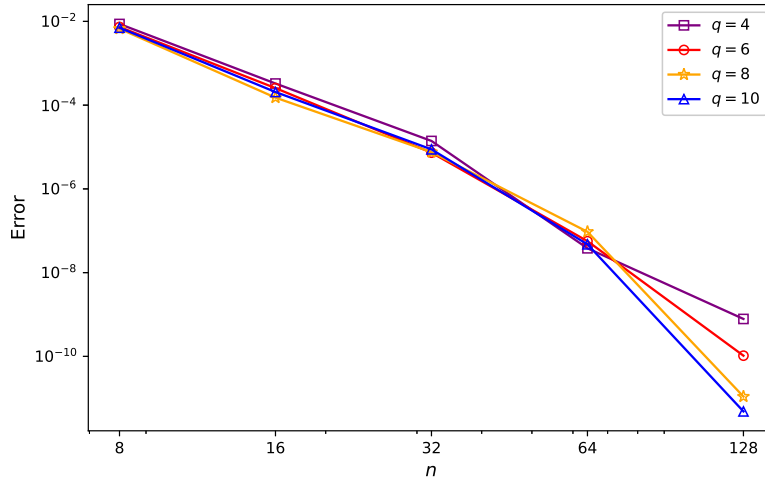


Fig. 8.3: Error of different order  $q$

**Test 4: Area of a region above  $z = x^2 + y^2$ .** Consider the region  $[-1, 1]^2 \times [-1, 3]$  intersect with  $\{z > x^2 + y^2\}$ , here we choose  $F(x, y) = x^2 + y^2 - z$  and  $f(x, y) = 1$ . The exact result is  $\frac{28}{3}$ . We use our method, with  $q = 4, 6, 8, 10$ , to solve the integral. The error is plotted in the figure 8.4 as follows:

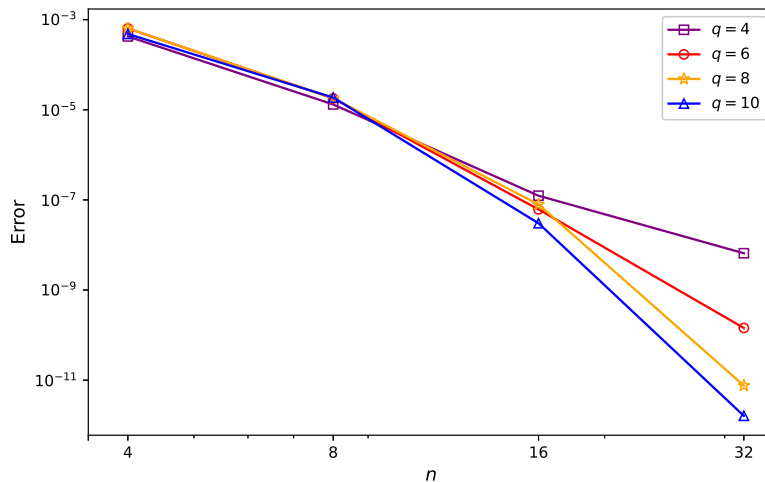


Fig. 8.4: Error of different order  $q$

**9. Conclusion and remarks** We present a novel high order numerical method for integral over smooth surfaces in  $\mathbb{R}^3$ . The key ingredient is to introduce the refine and displacement procedure to adjust the mesh to make sure the surface only has simple intersection with the mesh. Then the integral over each small intersections is easy to compute. Moreover, the effectiveness of the mesh adjustment procedure is rigorously proved. The proposed quadrature algorithm is easy to implement and very efficient, only need to solve a  $d$  dimensional linear system to get strictly positive quadrature weights and quadrature nodes. The numerical tests show that this algorithm is indeed higher order.

There are still many works we can do subsequently. In this paper, the surface is given by a level-set function. We can also consider the surfaces represented by unstructured point cloud. Furthermore, the proposed method can be used to solve PDEs on surfaces and interface problems.

**Acknowledgments.** This work is under the supervision of Prof. Zuoqiang Shi of Tsinghua University.

#### REFERENCES

- [1] L. BECK AND F. KUMMER, *High-order numerical integration on domains bounded by intersecting level sets*, arXiv preprint arXiv:2308.10698, (2023).
- [2] T. CUI, W. LENG, H. LIU, L. ZHANG, AND W. ZHENG, *High-order numerical quadratures in a tetrahedron with an implicitly defined curved interface*, ACM Transactions on Mathematical Software (TOMS), 46 (2020), pp. 1–18.
- [3] L. DRESCHER, H. HEUMANN, AND K. SCHMIDT, *A high order method for the approximation of integrals over implicitly defined hypersurfaces*, SIAM Journal on Numerical Analysis, 55 (2017), pp. 2592–2615.
- [4] H. FEDERER, *Curvature measures*, Transactions of the American Mathematical Society, 93 (1959), pp. 418–491, <http://www.jstor.org/stable/1993504> (accessed 2025-05-22).
- [5] T. P. FRIES AND S. OMERović, *Higher-order accurate integration of implicit geometries*, International Journal for Numerical Methods in Engineering, 106 (2016), pp. 323–371.
- [6] C. MIN AND F. GIBOU, *Geometric integration over irregular domains with application to level-set methods*, Journal of Computational Physics, 226 (2007), pp. 1432–1443.
- [7] C. MIN AND F. GIBOU, *Robust second-order accurate discretizations of the multi-dimensional heaviside and dirac delta functions*, Journal of Computational Physics, 227 (2008), pp. 9686–9695.
- [8] B. MÜLLER, F. KUMMER, AND M. OBERLACK, *Highly accurate surface and volume integration for level set methods using a moment-fitting approach*, Order, 6 (2013), pp. 10–16.
- [9] B. MÜLLER, F. KUMMER, AND M. OBERLACK, *Highly accurate surface and volume integration on implicit domains by means of moment-fitting*, International Journal for Numerical Methods in Engineering, 96 (2013), pp. 512–528.
- [10] M. A. OLSHANSKII AND D. SAFIN, *Numerical integration over implicitly defined domains for higher order unfitted finite element methods*, Lobachevskii Journal of Mathematics, 37 (2016), pp. 582–596.
- [11] B. A. PAYNE AND A. W. TOGA, *Surface mapping brain function on 3d models*, IEEE Computer Graphics and Applications, 10 (2002), pp. 33–41.
- [12] R. I. SAYE, *High-order quadrature methods for implicitly defined surfaces and volumes in hyperrectangles*, SIAM Journal on Scientific Computing, 37 (2015), pp. A993–A1019.
- [13] P. SMERKA, *The numerical approximation of a delta function with application to level set methods*, Journal of Computational Physics, 211 (2006), pp. 77–90.
- [14] J. D. TOWERS, *Two methods for discretizing a delta function supported on a level set*, Journal of Computational Physics, 220 (2007), pp. 915–931.
- [15] L. WE, *Marching cubes: A high resolution 3d surface construction algorithm*, Computer graphics, 21 (1987), pp. 7–12.
- [16] X. WEN, *High order numerical quadratures to one dimensional delta function integrals*, SIAM Journal on Scientific Computing, 30 (2008), pp. 1825–1846.
- [17] X. WEN, *High order numerical methods to two dimensional delta function integrals in level set methods*, Journal of Computational Physics, 228 (2009), pp. 4273–4290.

- [18] X. WEN, *High order numerical methods to three dimensional delta function integrals in level set methods*, SIAM Journal on Scientific Computing, 32 (2010), pp. 1288–1309.
- [19] S. ZAHEDI AND A.-K. TORBERG, *Delta function approximations in level set methods by distance function extension*, Journal of Computational Physics, 229 (2010), pp. 2199–2219.